Monthly Notices of the ROYAL ASTRONOMICAL SOCIETY

MNRAS **525,** 5492–5499 (2023) https://doi.org/10.1093/mnras/stad2628
Advance Access publication 2023 September 1

Probing the impact of WIMP dark matter on universal relations, GW170817 posterior, and radial oscillations

Pinku Routaray,[1] Abdul Quddus [2]★ Kabir Chakravarti[3,4] and Bharat Kumar[1]★

[1]Department of Physics and Astronomy, National Institute of Technology, Rourkela 769008, India
[2]Applied Sciences and Humanities Section, University Polytechnic, Aligarh Muslim University, Aligarh 202002, India
[3]Inter-University Centre for Astronomy and Astrophysics, Pune 411007, India
[4]Indian Institute of Technology, Gandhinagar 382055, India

Accepted 2023 August 24. Received 2023 August 19; in original form 2023 May 20

ABSTRACT

In this study, we investigate the impact of weakly interacting massive particles (WIMPs) dark matter (DM) on C–Λ universal relations, GW170817 posterior, and radial oscillations of neutron stars (NSs) by considering the interactions of uniformly trapped neutralinos as a DM candidate with the hadronic matter through the exchange of the Higgs boson within the framework of the Next-to-Minimal Supersymmetric Standard Model (NMSSM). The hadronic equation of state (EOS) is modelled using the relativistic mean-field (RMF) formalism with IOPB-I, G3, and quark–meson coupling (QMC)-RMF series parameter sets. The presence of DM softens the EOS at both the background and the perturbation levels that implies a small shift to the left in the posterior accompanied by a much larger jump in the left of the mass–radius curves with increasing DM mass. It is observed that EOSs with DM also satisfy the C–Λ universality relations among themselves but get slightly shifted to the right in comparison to that without considering DM. Additionally, we find that the inclusion of DM allows the mass–radius (M–R) curves to remain consistent with observational constraints for HESS J1731−347, indicating the possibility of classifying it as a dark matter-admixed neutron star (DMANS). Moreover, we explore the impact of DM on the radial oscillations of pulsating stars and investigate the stability of NSs. The results demonstrate a positive correlation between the mass of DM and the frequencies of radial oscillation modes.

Key words: gravitational waves – stars: neutron – dark matter – neutron star mergers.

1 INTRODUCTION

GW170817, the first discovery of gravitational waves (GWs) from the merger of binary neutron stars (BNS; Abbott et al. 2017), has provided a new methodology to constrain an equation of state (EOS) – a definitive relation between pressure and energy density – of neutron star (NS; Annala et al. 2018). A second signal GW190425, likely emitted during an NS binary coalescence, is originated from a much greater distance (Abbott et al. 2020) and thus much weaker than GW170817. However, the presence of NSs in the binary cannot be established beyond doubt. None the less, possible upcoming detections of such a post-merger signal (Torres-Rivas 2019) will put forward yet another macroscopic probe of NS physics (e.g. Bauswein 2015; Baiotti & Rezzolla 2017). The mass constraints put by the GW170817 data ($2.01 \pm 0.04 \lesssim M\,(\mathrm{M}_\odot) \lesssim 2.16 \pm 0.03$; Rezzolla, Most & Weih 2018) and the experimental measured mass of PSR J0348+0432 (with mass $2.01 \pm 0.04\ \mathrm{M}_\odot$; Antoniadis et al. 2013) propound that NSs should have the masses in the limit $\sim$2.0 M$_\odot$. The *Neutron Star Interior Composition Explorer* (*NICER*) observation constrains the radius of an NS to be in the range 11.96–14.26 km (Miller et al. 2019). Recently, astronomers made an interesting discovery within the remains of a supernova explosion: a central compact object (CCO) has been seen and named HESS J1731−347 (Doroshenko et al. 2022). This mysterious object shows a mass of about $0.77^{+0.20}_{-0.17}\ \mathrm{M}_\odot$ and a radius estimated to be approximately $10.4^{+0.86}_{-0.78}$ km. The unexpected features of HESS J1731−347 have sparked a lively discussion among scientists, focusing on its true nature. The newly found object's characteristics have raised an intriguing question: is it an NS with an extremely low mass, or could it be a strange star, displaying a more exotic EOS (Di Clemente, Drago & Pagliara 2022; Das & Lopes 2023; Horvath et al. 2023; Huang et al. 2023; Kubis et al. 2023; Rather, Panotopoulos & Lopes 2023; Sagun et al. 2023)? The nature of this compact object is still concealed in mystery, and further observations and thorough studies are needed to uncover its true identity.

The marvellous combination of low temperatures and supranuclear densities, unattended anywhere else in the Universe, makes NSs coveted and peerless laboratories for testing such extreme matter. With the establishment of GW astronomy on a firm observational footing, it is now plausible to comprehend and, better still, probe primal queries of nature. For example, recently in Chakravarti et al. (2020), the effect of introducing extra dimensions on NS properties has been studied, and the brane tension in the brane-world model is constrained using the GW170817 posterior. Potential forthcoming BNS inspirals, merger, and post-merger data can be used to test alterations in general relativity with finite-range scalar forces (in particular, $f(r)$ gravity) (Sagunski 2018). The observation of GWs

★ E-mail: abdulquddusphy@gmail.com (AQ); kumarbh@nitrkl.ac.in (BK)

from the BNS merger can also shed light on a plausible model of dark matter (DM) that could yield some extra peaks in the post-merger frequency spectrum. These peaks can be detected in the foreseeable time GWs signal from NS mergers (Ellis et al. 2018). Hence, NSs are a sensitive probe to detect and define the nature of DM particles.

Astrophysical constraints on the masses and radii of NSs have long been used to comprehend the microscopic properties of the matter that forms them. Since the first evidence of the 'missing mass' problem (Zwicky 1933, 2009), a lot of theoretical, experimental, and observational efforts have been made to solve the mystery of DM. The nature and origin of DM particles are still unknown, nevertheless, many DM candidates (for a review on DM candidates, see e.g. Taoso, Bertone & Masiero 2008) have been proposed and examined to constrain their properties. An enthralling solution to the DM case is given by weakly interacting massive particles (WIMPs; Muñoz 2004 and references therein), which satisfy the relic density of DM in the Universe (calculated by the WMAP Collaboration: 0.094 $\leq$ relic density $\leq$ 0.129, Bennett et al. 2003; Spergel et al. 2003; and the Planck Collaboration: 0.120 $\pm$ 0.001, Planck Collaboration VI 2020). However, WIMPs are very arduous to detect, yet their interactions with nuclei through elastic (Muñoz 2004) or inelastic scattering (Ellis, Flores & Lewin 1988; Ejiri, Fushimi & Ohsumi 1993; Starkman 1995) are being studied in several laboratories. Experiments for the direct detection of DM, such as Large Underground Xenon (LUX), XENON, and DArk MAtter/Large sodium Iodide Bulk for RAre processes (DAMA/LIBRA), impose stringent constraints on the parameter space of DM particles. The stiffest bound on the WIMP–nucleon spin-independent cross-section achieved by the LUX (Frederico Pascoal da Silva 2017), XENON (Aprile et al. 2017), and DAMA/LIBRA (Belli 2011; Bernabei et al. 2019) collaborations are, respectively, 1.1 $\times$ 10^{-46} cm^2 for 50 GeV/c^2 WIMPs, 7.7 $\times$ 10^{-47} cm^2 for 35 GeV/c^2 WIMPs, and $\sim$$10^{-40}$ cm^2 for 10 GeV/c^2 WIMPs at 90 per cent confidence level. The invisible Higgs decay width, provided by the A Toroidal LHC ApparatuS (ATLAS) and Compact Muon Solenoid (CMS) collaborations at the Large Hadron Collider (LHC), strongly constraint the DM below $m_h/2$ (m_h: Higgs mass), hence, kinematically favourable for Higgs boson to decay into pair of DM particle with mass M_{DM} < 62.5 GeV (Lopes 2022). Indirect searches for DM also constrain its mass. The mass of WIMP is constrained in the range of few eV < M_{DM} < 1 MeV with the help of the data on the age, density, and observed structure of the present universe (Steigman & Turner 1985). In Bringmann (2014), the thermal annihilation rate is constrained with the value $\langle\sigma v\rangle = 3 \times 10^{-26}$ cm^3 s^{-1} for DM masses $M_{DM} \leq 100$ GeV ($M_{DM} \leq 200$ GeV) assuming cardinal annihilation to $\mu^+\mu^-$ (e^+e^-) final states and for $M_{DM} \leq 35$ GeV ($M_{DM} \leq 55$ GeV) considering chief annihilation into light quarks ($b\bar{b}$).

Apart from DM direct/indirect detections (Gascon 2015; Gaskins 2016; Kahlhoefer 2017), constraints on DM parameters can also be set by observations of NS properties (Goldman 1989; Gould et al. 1990; Bertone 2008; Kouvaris 2008, 2010, 2011; de Lavallaz & Fairbairn 2010; Leung 2011; McDermott 2012; Bramante 2013, 2014, 2022; Güver et al. 2014; Baryakhtar 2017; Baym 2018; Ellis 2018; Ellis et al. 2018; Hook & Huang 2018; McKeen 2018; Raj 2018; Huang 2019; Ivanytskyi 2020; Karkevandi 2022). These studies are done by considering WIMPs trapped inside NS (Goldman 1989), studying effects of self-interacting/annihilating DM on NS (Kouvaris 2008, 2010; Lavallaz 2010; Bramante 2013, 2014; Ellis 2018; Karkevandi 2022), the impact of charged massive DM particle on NSs (Gould et al. 1990), probing axions with NS mergers (Hook & Huang 2018; Huang 2019), and from the collapse of an NS due to accretion of non-annihilating DM (Kouvaris 2011; Leung 2011; McDermott 2012; Güver et al. 2014) etc. In Nelson, Reddy & Zhou (2019) and Karkevandi (2022), the DM parameters are constrained by considering DM halo around NS. The effects of DM (WIMPs trapped inside an NS core) on NS properties have been studied (Panotopoulos 2017; Das 2019; Quddus et al. 2020) within the relativistic mean-field (RMF) formalism. Considering the mechanical model of the DM core inside an NS, it is shown in Ellis et al. (2018) that supplementary peaks may be observed in the power spectral density (PSD) of the GW emission following an NS–NS merger. In Das, Malik & Nayak (2020a), the unknown parameters of the DM EOS are fixed by using Bayesian parameter optimization. Recently, the mass of a fermionic DM particle (M_{DM} $\sim$ 60 GeV for a 2 $M_\odot$ NS) with its fraction inside an NS is constrained by using data on the spatial distribution of DM in the Milky Way and following the two-fluid approach (DM and NS matter interact gravitationally; Ivanytskyi 2020). Moreover, in Karkevandi (2022), it is found that considering bosonic DM inside the NS core and imposing constraints from NS observable mass and tidal deformability data by the LIGO/Virgo Collaboration, sub-GeV DM particles are favoured with a low fraction below $\sim$5 per cent. In addition, another crucial microscopic property known as the oscillation of an NS plays a significant role in investigating the NS internal composition and serves as a valuable constraint for understanding the EOS. These oscillations can occur in two ways: radial and non-radial oscillations. Over the years, numerous studies have been proposed to elucidate the phenomenon of NS oscillation (Chandrasekhar 1964; Chanmugam 1977; Vaeth & Chanmugam 1992; Gondek, Haensel & Zdunik 1997; Gondek & Zdunik 1999; Kokkotas & Ruoff 2001; Kunjipurayil et al. 2022; Sen et al. 2023), each assuming different compositions of the NS. Therefore, in our dark matter-admixed neutron star (DMANS) model, the impact of DM on the oscillations is studied.

In this study, we have considered the presence of WIMPs trapped inside the NS core. The detection of theoretically predicted peaks in the post-merger frequency spectrum (Ellis et al. 2018) may provide valuable insights into the nature of DM. However, at the present time, the LIGO–Virgo–KAGRA detectors are still far from achieving the required sensitivity to fully solve the DM puzzle. As discussed, various theoretical studies (Kouvaris 2011; Panotopoulos 2017; Ellis 2018; Ellis et al. 2018; Das 2019; Das et al. 2020b; Ivanytskyi 2020; Quddus et al. 2020; Karkevandi 2022; Routaray et al. 2023a,b,c) lend support to the idea of a DM core existing inside an NS, but the DM parameters exhibit a significant degree of degeneracy. In this work, we present a posterior GW mass–radius (*M*–*R*) contour, developed using data from BNS mergers, to assess which *M*–*R* plots (obtained at different WIMP masses) are consistent with the observational data. Additionally, we utilize the mass–radius constraint of the CCO HESS J1731−347 to determine its true nature within the DMANS model. The C–Λ universality relations (where C is the compactness of a star and Λ is its dimensionless tidal deformability) have been discussed for the EOSs corresponding to these different WIMP masses to investigate whether this universality breaks down with DM presence (and on increasing its mass) or not.

2 EQUATION OF STATE OF DARK MATTER-ADMIXED NEUTRON STAR

The presence of a DM core inside an NS with a mass fraction of approximately $\sim$5 per cent has significant effects on NS data (Ellis 2018). The amount of DM present inside an NS is not universal; instead, it depends on the environment in which the NS was formed and its evolution history (age and initial temperature; Ellis 2018). For the usual evolution of an NS with a lifetime of approximately ∼10 Gyr, the accreted WIMP DM amount does not exceed $\sim 10^{-10}$ M$_\odot$ (Goldman 1989; Kouvaris 2008, 2010; Güver et al. 2014). The formation of adequate DM cores or haloes would require additional mechanisms, such as the conversion of neutrons to scalar DM (Ellis 2018), scalar DM production via the neutron bremsstrahlung process (Ellis 2018; Nelson et al. 2019), or gravitational interaction of the NS with a DM star (Foot 2004; Fan et al. 2013; Pollack, Spergel & Steinhardt 2015; Ellis 2018). It has been shown in Brayeur (2012) that BNS mergers might increase the probability of DM agglomeration inside the NS.

In this study, we have considered the interaction of neutralino (χ) – the lightest mass eigenstate of WIMP within the Next-to-Minimal Supersymmetric Standard Model (NMSSM; Gunion, Belikov & Hooper 2010) – as one of the fermionic DM candidates. We assume that the neutralino interacts with the hadronic part of the NS through the exchange of the Higgs field h. It is important to note that the obtained results and analyses remain valid for any fermionic WIMP. The reason for considering the WIMP as a DM candidate is that a one-to-one relation is observed between the spin-independent direct detection rate and the DM relic density if the elastic scattering on nuclei occurs dominantly through Higgs exchange (Andreas, Hambye & Tytgat 2008).

The NMSSM (Ellwanger, Rausch de Traubenberg & Savoy 1993, 1995, 1997; Maniatis 2010) is a simple extension of the Minimal Supersymmetric Standard Model (MSSM) with the addition of a singlet supermultiplet. It offers several advantages over the MSSM.

(i) It provides a solution to the hierarchy problem while preserving the favourable properties of the MSSM.
(ii) It addresses the μ problem (Kim & Nilles 1984).
(iii) Compared to the MSSM, NMSSM introduces two additional Higgs bosons.

It is noteworthy that in NMSSM (Bae, Kim & Shin 2010; Gunion et al. 2010), the spin-independent cross-section of DM–nucleon scattering can be as high as the one implied by the DAMA results (Andreas et al. 2008). This is in contrast to the MSSM, where such high cross-sections are not achievable due to the absence of light Higgs bosons exchange. However, it should be mentioned that the DAMA results have faced significant criticism (Buttazzo et al. 2020), and other similar experiments have not confirmed any signal yet (Amaré et al. 2020). In this work, we propose to analyse the effect of this region of the parameter space on the properties of NSs. The interaction Lagrangian density for the neutralino interacting with the hadronic matter of nuclear matter (NM), φ, through Higgs exchange is given as follows:

$$\mathcal{L} = \mathcal{L}_{\rm had.} + \bar{\chi}\left[i\gamma^\mu\partial_\mu - M_{\rm DM} + yh\right]\chi + \frac{1}{2}\partial_\mu h\partial^\mu h - \frac{1}{2}M_{\rm h}^2h^2 + f\frac{M_{\rm n}}{v}\bar{\varphi}h\varphi, \quad (1)$$

where $\mathcal{L}_{\rm had.}$ is the Lagrangian density for the hadronic matter (for details, see Quddus et al. 2020). The factor f represents the Higgs–nucleon coupling parameter (Cline 2013, 2015), with a central value $f = 0.3$ considered based on lattice computations (Ren et al. 2012; Alarcón, Martin Camalich & Oller 2013; Alvarez-Ruso et al. 2013; Young 2013). In this context, $M_{\rm n}$ and $M_{\rm h}$ denote the masses of the nucleon and Higgs boson, respectively, and $v = 246$ GeV corresponds to the Higgs vacuum expectation value. Within NMSSM, a light Higgs boson with mass $M_{\rm h}$ = 40 GeV is chosen to satisfy the condition that the Yukawa coupling (interaction strength of the Higgs field with the DM particles) remains in the perturbative regime ($y < 1$). On changing the DM particle mass, the coupling coefficient y is calculated by following the equation:

$$\sigma(\chi\varphi \to \chi\varphi) = \frac{y^2}{\pi}\frac{\mu^2}{v^2m_{\rm h}^4}f^2M_{\rm n}^2, \quad (2)$$

where μ is the reduced mass of a DM–nucleon system, and σ is the spin-independent cross-section of DM interaction with nucleon, satisfying the DAMA results (Andreas et al. 2008).

The EOS of NM can be derived within effective theories that incorporate appropriate degrees of freedom. Various approaches, such as non-relativistic Skyrme-type density functional theory (Tondeur et al. 1984), perturbative quantum chromodynamics (QCD; Kurkela 2010; Gorda 2016), and the RMF (Walecka 1974), are used to generate EOSs of NM. In this study, we have generated EOSs of pure hadronic matter using the RMF formalism. These EOSs correspond to the parameter sets IOPB-I (Kumar 2018), G3 (Kumar et al. 2017), quark–meson coupling (QMC)-RMF1, QMC-RMF2, QMC-RMF3, and QMC-RMF4 (Alford et al. 2022). The QMC-RMF series of parameter sets are specifically developed to model NM across a wide range of temperatures and densities that are relevant for NSs and NS mergers. These interactions take into account the uncertainties provided by chiral effective field theory (χEFT) for neutron matter and are consistent with contemporary astrophysical constraints on the EOS (Alford et al. 2022).

By considering the RMF EOS for the hadronic part of the NS and imposing charge neutrality and chemical equilibrium conditions, the EOS of a dark matter-admixed neutron star (DMANS) can be determined using mean-field approximations and the variational principle. The detailed formalism can be found in Quddus et al. (2020), but for completeness, we provide here the expressions for the energy density and pressure of the DMANS:

$$\mathcal{E}_{\rm NS} = \mathcal{E}_{\rm had.} + \mathcal{E}_{\rm DM} + \mathcal{E}_{\rm l}, \qquad P_{\rm NS} = P_{\rm had.} + P_{\rm DM} + P_{\rm l}, \quad (3)$$

where

$$\mathcal{E}_{\rm l} = \sum_{l=e,\mu}\frac{2}{(2\pi)^3}\int_0^{k_{\rm l}} {\rm d}^3k\sqrt{k^2+m_{\rm l}^2}, \qquad P_{\rm l} = \sum_{l=e,\mu}\frac{2}{3(2\pi)^3}\int_0^{k_{\rm l}}\frac{{\rm d}^3k k^2}{\sqrt{k^2+m_{\rm l}^2}} \quad (4)$$

are the energy density and pressure for the leptonic part of an NS with leptonic mass $m_{\rm l}$, and Fermi momentum $k_{\rm l}$,

$$\mathcal{E}_{\rm DM} = \frac{2}{(2\pi)^3}\int_0^{k_{\rm F}^{\rm DM}} {\rm d}^3k\sqrt{k^2+(M_{\rm DM}^\star)^2} + \frac{1}{2}M_{\rm h}^2h_0^2, \qquad P_{\rm DM} = \frac{2}{3(2\pi)^3}\int_0^{k_{\rm F}^{\rm DM}}\frac{{\rm d}^3k k^2}{\sqrt{k^2+(M_{\rm DM}^\star)^2}} - \frac{1}{2}M_{\rm h}^2h_0^2 \quad (5)$$

are the expressions for energy density and pressure for the DM interaction with the hadronic matter of an NS through the exchange of Higgs field with DM Fermi momentum $k_{\rm F}^{\rm DM} = 0.06$ GeV (Das 2019; Quddus et al. 2020), assuming baryonic density of NS about 10^3 times greater than the DM density inside NS. The energy density and pressure for the hadronic part of NS are given as the following:

$$\begin{aligned}\mathcal{E}_{\rm had.} =& \frac{2}{(2\pi)^3}\int d^3k E_i^*(k) + \rho_b W + \frac{m_s^2\Phi^2}{g_s^2}\left(\frac{1}{2}+\frac{\kappa_3}{3!}\frac{\Phi}{M}\right.\\ &\left.+\frac{\kappa_4}{4!}\frac{\Phi^2}{M^2}\right) - \frac{1}{2}m_\omega^2\frac{W^2}{g_\omega^2}\left(1+\eta_1\frac{\Phi}{M}+\frac{\eta_2}{2}\frac{\Phi^2}{M^2}\right)\\ &-\frac{1}{4!}\frac{\zeta_0 W^4}{g_\omega^2}+\frac{1}{2}\rho_3 R - \frac{1}{2}\left(1+\frac{\eta_\rho\Phi}{M}\right)\frac{m_\rho^2}{g_\rho^2}R^2\\ &-\Lambda_\omega(R^2\times W^2)+\frac{1}{2}\frac{m_\delta^2}{g_\delta^2}\left(D^2\right),\\ P_{\rm had.} =& \frac{2}{3(2\pi)^3}\int d^3k\frac{k^2}{E_i^*(k)} - \frac{m_s^2\Phi^2}{g_s^2}\left(\frac{1}{2}+\frac{\kappa_3}{3!}\frac{\Phi}{M}\right.\\ &\left.+\frac{\kappa_4}{4!}\frac{\Phi^2}{M^2}\right)+\frac{1}{2}m_\omega^2\frac{W^2}{g_\omega^2}\left(1+\eta_1\frac{\Phi}{M}+\frac{\eta_2}{2}\frac{\Phi^2}{M^2}\right)\\ &+\frac{1}{4!}\frac{\zeta_0 W^4}{g_\omega^2}+\frac{1}{2}\left(1+\frac{\eta_\rho\Phi}{M}\right)\frac{m_\rho^2}{g_\rho^2}R^2\\ &+\Lambda_\omega(R^2\times W^2)-\frac{1}{2}\frac{m_\delta^2}{g_\delta^2}\left(D^2\right), \end{aligned} \quad (6)$$

where $\Phi, D, W,$ and R are the redefined fields for $\sigma, \delta, \omega,$ and ρ mesons (see Quddus et al. 2020), while $E_i^*(k) = \sqrt{k^2 + M_i^{*2}}$ $(i = p, n)$ is the energy with effective mass $M_i^{*2} = k_F^2 + M_i^2$, and k is the momentum of the nucleon. The quantities ρ_b and ρ_3 in the above equation have their usual meanings as the baryonic and isoscalar densities, respectively. Because of the presence of Higgs field, the effective mass of nucleon get modified as $M_i^\star = M_i + g_\sigma\sigma - \tau_3 g_\delta\delta - \frac{fM_n}{v}h_0$, while the DM effective mass is $M_{\rm DM}^\star = M_{\rm DM} - yh_0$, where h_0 is the time component of Higgs field. Putting equation (3) in the Tolman–Oppenheimer–Volkoff (TOV) equations (Oppenheimer 1939; Tolman 1939) gives the mass–radius profile of NS.

3 RADIAL OSCILLATIONS

To analyse the equations governing the radial oscillations of NS, we introduce the variable $\delta r(r, t)$, representing the time-varying radial displacement of a fluid element,

$$\delta r(r,t) = X(r)\,e^{i\omega t}. \quad (7)$$

The variable $X(r)$ represents the amplitude, while ω denotes the circular frequency of the standing wave solution. The linearized perturbation equation is mathematically represented as shown by Kokkotas & Ruoff (2001) and Sen et al. (2023),

$$\begin{aligned} &c_s^2 X'' + \left(\left(c_s^2\right)' - Z + \frac{4\pi G}{c^4} r\gamma P e^{2\lambda} - \nu' c^2\right)X'\\ &+\left[2\left(\nu'\right)^2 c^2 + \frac{2Gm}{r^3}e^{2\lambda} - Z' - \frac{4\pi G}{c^4}(P+\mathcal{E})Zre^{2\lambda}\right]X\\ &+\omega^2 e^{2\lambda-2\nu}X = 0. \end{aligned} \quad (8)$$

The variable c_s^2 represents the square of the speed of sound, while γ denotes the adiabatic index. Here, $e^{2\lambda(R)} = \left(1 - \frac{2GM}{c^2R}\right)^{-1}$ is the metric function and $Z(r) = \left(\nu' - \frac{2}{r}\right)c_s^2$. And for the numerical solution, we use $\mathcal{E} = \mathcal{E}_{\rm NS}$ and $P = P_{\rm NS}$ from equation (3).

The boundary conditions for the equations governing oscillations must be formulated to ensure zero displacement at the centre ($\delta r(r = 0) = 0$), while also guaranteeing that the Lagrangian perturbation of pressure becomes zero at the surface ($\Delta P(r = R) = 0$).

Considering the mentioned boundary conditions, the displacement function can be rewritten as follow:

$$\zeta = r^2 e^{-\nu} X. \quad (9)$$

By introducing the above new variable, the equation (8) can be reformulated as a Sturm–Liouville differential equation that possesses a self-adjoint characteristic,

$$\frac{d}{dr}\left(H\frac{d\zeta}{dr}\right) + \left(\omega^2 W + Q\right)\zeta = 0, \quad (10)$$

where

$$\begin{aligned} r^2 H &= (P+\mathcal{E})\,e^{\lambda+3\nu}c_s^2,\\ r^2 W &= (P+\mathcal{E})\,e^{3\lambda+\nu},\\ r^2 Q &= (P+\mathcal{E})\,e^{\lambda+3\nu}\left((\nu')^2 + \frac{4}{r}\nu' - \frac{8\pi G}{c^4}e^{2\lambda}P\right). \end{aligned} \quad (11)$$

The equation labelled as (10) represents the fundamental equation governing radial oscillations. In this equation, the quantity ΔP takes a simple expression given by $\Delta P = -r^{-2}e^{\nu}(P+\mathcal{E})c_s^2\zeta'$.

Furthermore, it is worth noting that equation (10) can be expressed in the Sturm–Liouville form. In this representation, the function ζ_n exhibits n nodes between the surface and the centre and possesses discrete eigenvalues denoted as ω_n^2. These eigenvalues follow a specific structure,

$$\omega_0^2 < \omega_1^2 < \cdots < \omega_n^2 < \cdots.$$

The solution represented by equation (7) indicates that oscillations exhibit harmonic behaviour and remain stable when the frequency ω is real. However, the star will experience instability when the frequency associated with the node is imaginary.

4 RESULTS AND DISCUSSIONS

In the literature, it is well known that there exist EOS independent relations (Yagi 2013; Yagi & Yunes 2013, 2017) among NSs. These relations hold true under various circumstances, as long as we exclude cases where abrupt phase transitions occur within the star (Yagi & Yunes 2017). Of particular interest to us are the C–Λ universal relations, also referred to as Universal relations of the first kind. This relation can be expressed through the coefficients c_n of the polynomial fit,

$$C = \sum_{n=0}^{4} c_n\left(\log_{10}\Lambda\right)^n, \quad (12)$$

between C and $\log_{10}\Lambda$. In the presence of DM, both C and Λ undergo changes. The panels of Fig. 1 display the variation of C–Λ across different stellar configurations for four distinct values of DM particle masses. Interestingly, we observe that the sequence of C–Λ points deviates more as more massive DM is added, but *does not* break the qualitative nature of the universal behaviour. This enables us to fit C–Λ for each case of DM mass, and the corresponding fitting coefficients are presented in Table 1.

Since the frequency of GWs depends on the chirp mass and mass ratio, the mass M of an NS can be inferred from the observed phases of GWs. Similarly, the tidal deformability Λ of the NS can also be inferred from the GWs phase during the inspiraling process. Therefore, (M, Λ) can be considered as primary GW observables. Subsequently, the C–Λ universal relations are utilized to convert the raw M–Λ posterior into M–R posteriors (Abbott et al. 2017), which are extensively used in EOS inference. In the presence of DM, the modified nature of the C–Λ function results in a shift in the posterior

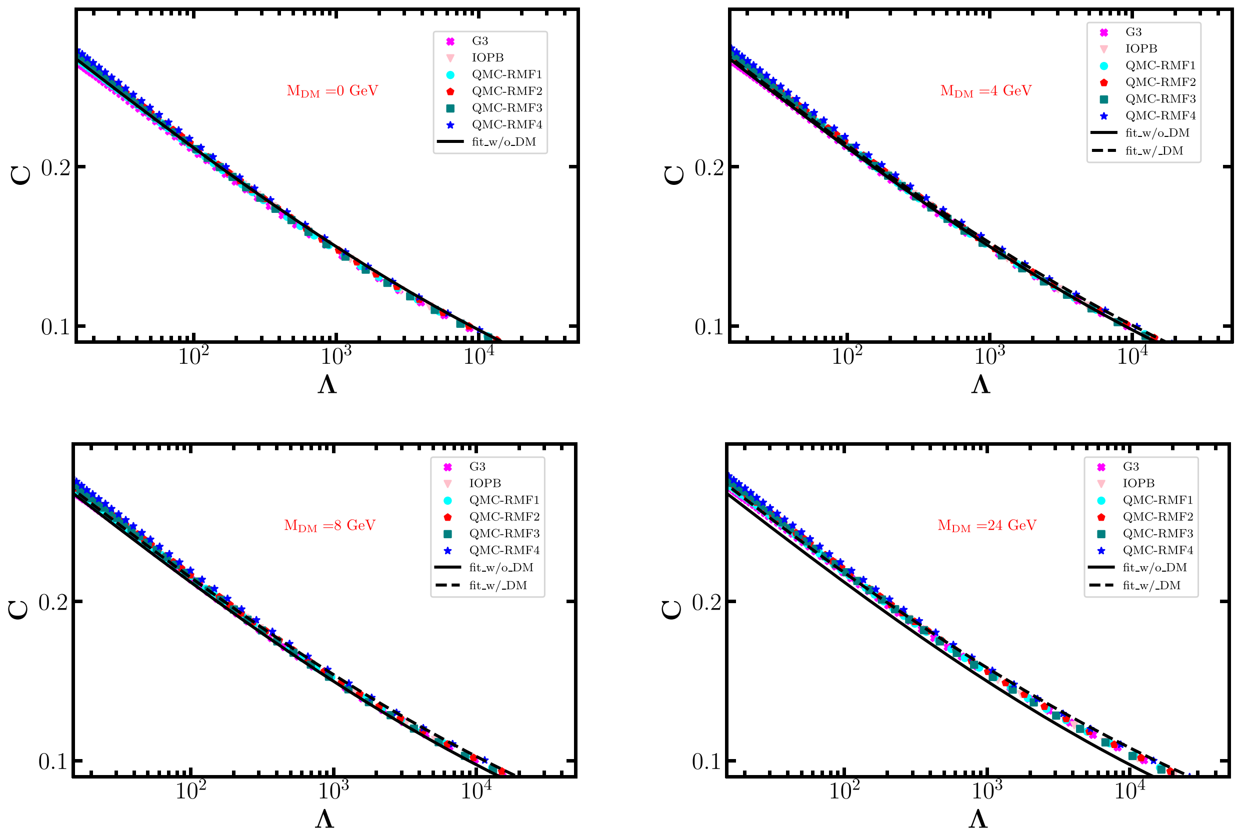

Figure 1. Universality relation for an NS corresponding to the chosen EOSs without DM is presented in the panel (a), followed by the same in the presence of DM with $M_{\rm DM} = 4$ GeV in panel (b), $M_{\rm DM} = 8$ GeV in panel (c), and $M_{\rm DM} = 24$ GeV in panel (d), respectively. The black bold line is the fitted curve of C–Λ relation when there is no DM presence. The sequence of C–Λ points deviate more as more massive DM is added, but does not break the qualitative nature of the universal behaviour and the corresponding fitted curves are represented by black dashed lines in panels (b)–(d).

Table 1. Fitting coefficients of C–Λ relation are shown along with reduced χ^2 value for different DM mass.

$M_{\rm DM}$ (GeV)	c_0	c_1	c_2	c_3	c_4	χ_r^2(1e-6)
0	0.34791	−0.06568	− 0.00358	0.00136	−6.90e-05	6.0516
4	0.35042	−0.06785	− 0.00232	0.00114	−5.82e-05	6.4963
8	0.35242	−0.06950	− 0.00140	9.97e-04	−5.07e-05	6.8681
24	0.35821	−0.07416	9.26e-04	6.27e-04	−3.31e-05	7.9838

in the M–R plane, making the EOSs softer, and the M–R curves shift to the left (Fig. 2). This shift also affects the posteriors (including the 90 per cent and the 50 per cent confidence level) as shown in Fig. 2. A somewhat similar effect was observed in Chakravarti et al. (2020), where the presence of extra dimensions resulted in a shift of the M–R curves and posteriors to the right. The effects of changing EOS due to DM are not only limited to the background properties of NSs but also extend to the perturbations, leading to variations in C for a given value of Λ (Fig. 1). Consequently, the posteriors shift accordingly in the M–R plane (Fig. 2). It is clearly evident that the shifting is more with higher DM mass. Another crucial observation from Fig. 2 is that the mass–radius profile satisfies the observational bound for HESS J1731−347 when DM is considered. Specifically, for $M_{\rm DM} = 24$ GeV, all the M–R curves satisfy this constraint. As a result, our study also refers the nature of HESS J1731−347 as a DMANS (Sagun et al. 2023).

In Fig. 3, we investigate the relationship between the eigenfrequencies and central ρ_c for the f-mode of radial oscillation. To accomplish this, we vary the mass of the DM using different models. As depicted in the corresponding figure, the stability limit is attained when the density increases and reaches the critical density, regardless of the EOS. At this critical point, the star reaches its maximum mass and becomes unstable, as indicated by a zero eigenvalue for the f-mode (Kokkotas & Ruoff 2001). However, as the mass of DM increases, the critical density also rises due to the softening of the EoS, resulting in higher frequency oscillations. When the density of the star exceeds the critical density, its oscillations exhibit exponential growth. Consequently, the star loses its ability to return to its initial state, ultimately undergoing gravitational collapse and forming a black hole.

Fig. 4 displays how the frequency of the f-mode changes with different NS masses, considering the presence and absence of DM, using various models. We observe that the behaviour of the f-mode rapidly approaches zero precisely at the point where the NS reaches its maximum mass. This finding aligns with the stability criteria $\partial M/\partial \rho_c > 0$, proposed by Harrison et al. (1965) and Shapiro & Teukolsky (1983), which indicate that the NS remains stable as its mass changes with respect to the ρ_c.

5 SUMMARY AND CONCLUSION

The primary objective of this work is to investigate the impact of WIMP DM on the C–Λ universal relation, GW170817 posteriors, and radial f-mode oscillation of NSs. We consider interactions of uniformly trapped neutralinos (the lightest WIMP) as a DM candidate with the hadronic matter of NSs through the exchange of the Higgs

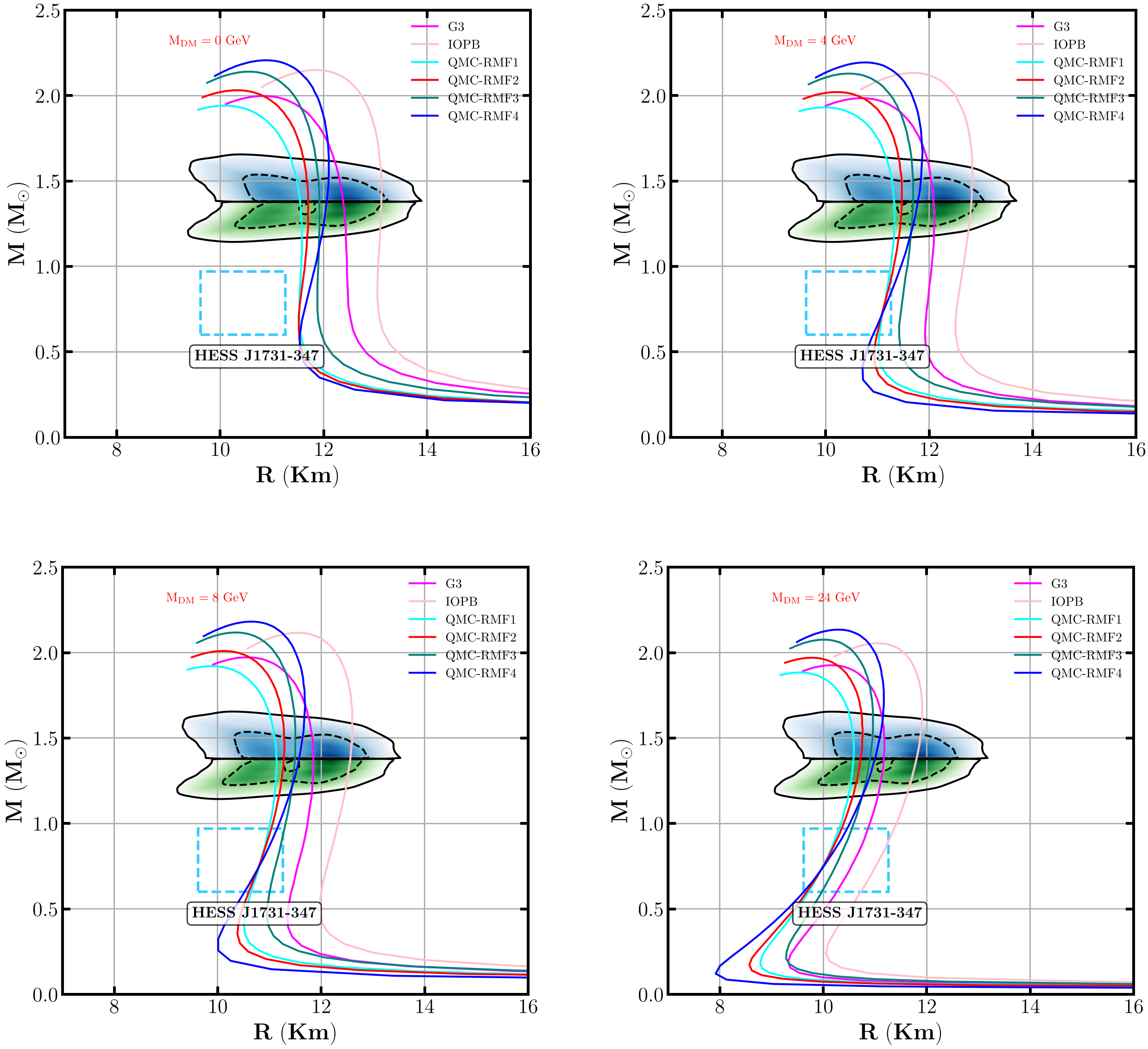

Figure 2. *M–R* curves of an NS corresponding to the chosen parameter sets in the absence of DM core (a) and in the presence of DM with $M_{\rm DM} = 4$ GeV (b), $M_{\rm DM} = 8$ GeV (c), and $M_{\rm DM} = 24$ GeV (d). The 90 per cent and 50 per cent confidence level posteriors for the primary (blue) and secondary (green) components of GW170817 are shown bounded by solid lines and dashed lines, respectively, in each panel. The dashed rectangular box shows the observational bound for HESS J1731−347.

boson, which is the lightest CP-even eigenstate of the NMSSM. The hadronic part of the EOS is modelled using RMF with IOPB-I, G3, and QMC-RMF series of parameter sets. The presence of DM inside the NS core results in reduced values of its properties, making the EOSs softer. The findings of this study can be summarized as follows.

(i) The EOSs with DM satisfy the universality relation of the first kind, the C–Λ universal relations, but they slightly shift to the right with increasing DM mass compared to the C–Λ universal relation when no DM is considered. However, the deviated curves satisfy universality relation among themselves.

(ii) A change in the mass of DM results in a small shift to the left in the posterior, accompanied by a much larger jump to the left in the *M–R* curves.

(iii) The incorporation of DM into the analysis allows the *M–R* curve to remain consistent with the mass–radius constraints imposed by HESS J1731−347. Therefore, this study contributes to determining the characteristics of HESS J1731−347, suggesting the possibility that it may be classified as a DMANS.

(iv) We further investigated the radial oscillations of pulsating stars by solving the Sturm–Liouville equations for the perturbations and imposing necessary boundary conditions. This allowed us to accurately determine the frequencies associated with the mode. The calculations for the fundamental *f*-mode were done with and without the presence of DM, while systematically varying the DM mass. The numerical findings indicate that the inclusion of DM within NSs leads to a reduction in the stiffness of the EOS, resulting in a decrease in the maximum mass of these stars. Additionally, the inclusion of DM leads to an increase in the frequencies of pulsating objects. In conclusion, there exists a positive correlation between the mass of the DM and the frequencies of the radial oscillation modes.

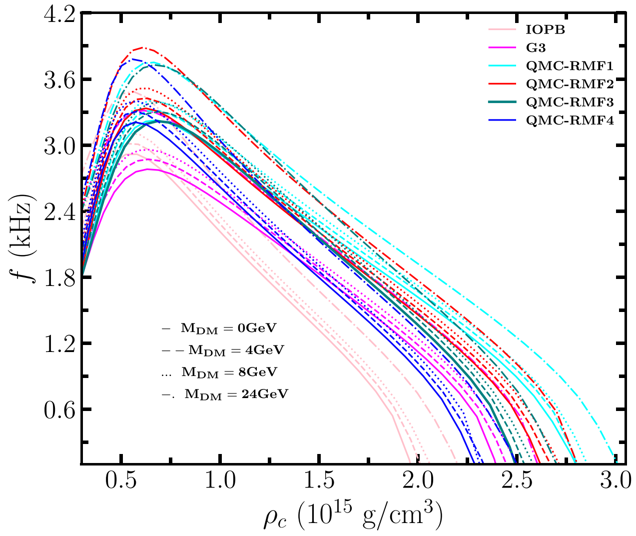

Figure 3. For different DM mass, the radial *f*-mode frequency is shown for G3, IOPB-I, and QMC-RMF series model with varying the central energy density (ρ_c).

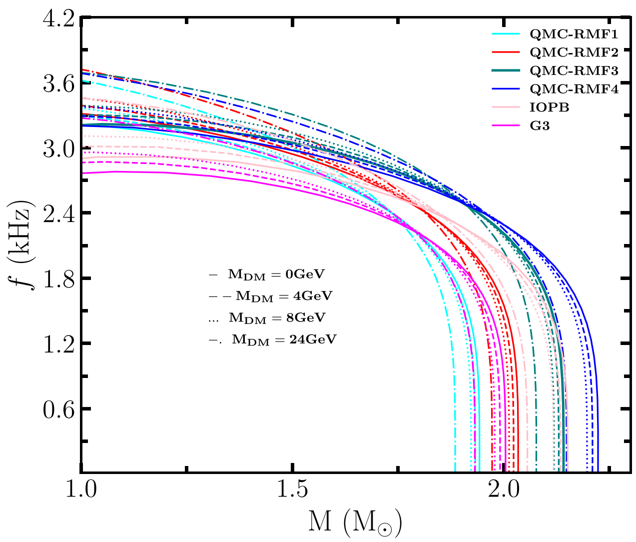

Figure 4. Behaviour of the *f*-mode frequency as a function of mass is plotted for different DM mass.

(v) Finally, we verified the stability criterion of NSs by studying the *f*-mode as a function of their mass.

ACKNOWLEDGEMENTS

We are grateful to Sukanta Bose for the discussion and enhancing the content of the paper. AQ is thankful to the IUCAA, Pune for providing nice hospitality during this work. AQ would like to thank S. K. Patra, Shakeb Ahmad, and Grigorios Panotopoulos for the nice discussion. The research of BK is supported by DST, India under a SERB CRG Grant with No. CRG/2021/000101.

DATA AVAILABILITY

The EOSs used in this paper can be inferred from their original articles cited above. Fitting coefficients for C–Λ universality relations are given in the text.

REFERENCES

Abbott B. P. et al., 2017, Phys. Rev. Lett., 119, 161101
Abbott B. P. et al., 2020, ApJ, 892, L3
Alarcón J., Martin Camalich J., Oller J. A., 2013, Ann. Phys., 336, 413
Alford M. G., Brodie L., Haber A., Tews I., 2022, Phys. Rev. C, 106, 055804
Alvarez-Ruso L., Ledwig T., Camalich J. M., Vicente-Vacas M. J., 2013, Phys. Rev. D, 88, 054507
Amaré J. et al., 2020, J. Phys. Conf. Ser., 1468, 012014
Andreas S., Hambye T., Tytgat M. H. G., 2008, J. Cosmol. Astropart. Phys., 10, 034
Annala E., Gorda T., Kurkela A., Vuorinen A., 2018, Phys. Rev. Lett., 120, 172703
Antoniadis J. et al., 2013, Science, 340, 448
Aprile E. et al., 2017, Phys. Rev. Lett., 119, 181301
Bae K. J., Kim H. D, Shin S., 2010, Phys. Rev. D, 82, 115014
Baiotti L., Rezzolla L., 2017, Rep. Progress Phys., 80, 096901
Baryakhtar M., 2017, Phys. Rev. Lett., 119, 131801
Bauswein A., 2015, Phys. Rev. D, 91, 124056
Baym G., 2018, Phys. Rev. Lett., 121, 061801
Belli P., 2011, Phys. Rev. D, 84, 055014
Bennett C. L. et al., 2003, ApJS, 148, 1
Bernabei R. et al., 2019, Nucl. Phys. At. Energy, 20, 317
Bertone G., 2008, Phys. Rev. D, 77, 043515
Bramante J., 2013, Phys. Rev. D, 87, 055012
Bramante J., 2014, Phys. Rev. D, 89, 015010
Bramante J., 2022, Phys. Rev. Lett., 128, 231801
Brayeur L., 2012, Phys. Rev. Lett., 109, 061301
Bringmann T., 2014, Phys. Rev. D, 90, 123001
Buttazzo D., Panci P., Rossi N., Strumia A., 2020, J. High Energy Phys., 2020, 137
Chakravarti K., Chakraborty S., Phukon K. S., Bose S., SenGupta S., 2020, Classical Quantum Gravity, 37, 105004
Chandrasekhar S., 1964, ApJ, 140, 417
Chanmugam G., 1977, ApJ, 217, 799
Cline J. M., 2013, Phys. Rev. D, 88, 055025
Cline J. M., 2015, Phys. Rev. D, 92, 039906
Das A., 2019, Phys. Rev. D, 99, 043016
Das H. C., Lopes L. L., 2023, MNRAS, 525, 3571
Das A., Malik T., Nayak A. C., 2020a, preprint (arXiv:2011.01318)
Das H. C., Kumar A., Kumar B., Biswal S. K., Nakatsukasa T., Li A., Patra S. K., 2020b, MNRAS, 495, 4893
de Lavallaz A., Fairbairn M., 2010, Phys. Rev. D, 81, 123521
Di Clemente F., Drago A., Pagliara G., 2022, preprint (arXiv:2211.07485)
Doroshenko V., Suleimanov V., Pühlhofer G., Santangelo A., 2022, Nat. Astron., 6, 1444
Ejiri H., Fushimi K., Ohsumi H., 1993, Phys. Lett. B, 317, 14
Ellis J., 2018, Phys. Rev. D, 97, 123007
Ellis J., Flores R., Lewin J., 1988, Phys. Lett. B, 212, 375
Ellis J., Hektor A., Hütsi G., Kannike K., Marzola L., Raidal M., Vaskonen V., 2018, Phys. Lett. B, 781, 607
Ellwanger U., de Traubenberg M. R., Savoy C. A., 1993, Phys. Lett. B, 315, 331
Ellwanger U., Rausch de Traubenberg M., Savoy C. A., 1995, Z. Phys. C: Part. Fields, 67, 665
Ellwanger U., Rausch de Traubenberg M., Savoy C., 1997, Nucl. Phys. B, 492, 21
Fan J., Katz A., Randall L., Reece M., 2013, Phys. Dark Universe, 2, 139
Foot R., 2004, Int. J. Mod. Phys. D, 13, 2161
Frederico Pascoal da Silva C., 2017, preprint (arXiv:1710.03572)
Gascon J., 2015, EPJ Web Conf., 95, 02004
Gaskins J. M., 2016, Contemporary Phys., 57, 496
Goldman I., 1989, Phys. Rev. D, 40, 3221
Gondek D., Zdunik J. L., 1999, A&A, 344, 117
Gondek D., Haensel P., Zdunik J. L., 1997, A&A, 325, 217
Gorda T., 2016, ApJ, 832, 28
Gould A., Draine B. T., Romani R. W., Nussinov S., 1990, Phys. Lett. B, 238, 337

Gunion J. F., Belikov A. V., Hooper D., 2010, preprint (arXiv:1009.2555)
Güver T., Erkoca A. E., Reno M. H., Sarcevic I., 2014, J. Cosmol. Astropart. Phys., 05, 013
Harrison B. K., Thorne K. S., Wakano M., Wheeler J. A., 1965, Gravitation Theory and Gravitational Collapse. Univ. Chicago Press, Chicago
Hook A., Huang J., 2018, J. High Energy Phys., 2018, 36
Horvath J. E., Rocha L. S., de Sá L. M., Moraes P. H. R. S., Barão L. G., de Avellar M. G. B., Bernardo A., Bachega R. R. A., 2023, A&A, 672, L11
Huang J., 2019, Phys. Rev. D, 99, 063013
Huang K., Hu J., Zhang Y., Shen H., 2023, preprint (arXiv:2306.04992)
Ivanytskyi O., 2020, Phys. Rev. D, 102, 063028
Kahlhoefer F., 2017, Int. J. Mod. Phys. A, 32, 1730006
Karkevandi D. R., 2022, Phys. Rev. D, 105, 023001
Kim J. E., Nilles H., 1984, Phys. Lett. B, 138, 150
Kokkotas K. D., Ruoff J., 2001, A&A, 366, 565
Kouvaris C., 2008, Phys. Rev. D, 77, 023006
Kouvaris C., 2010, Phys. Rev. D, 82, 063531
Kouvaris C., 2011, Phys. Rev. D, 83, 083512
Kubis S., Wójcik W., Alvarez Castillo D., Zabari N., 2023, preprint (arXiv:2307.02979)
Kumar B., 2018, Phys. Rev. C, 97, 045806
Kumar B., Singh S., Agrawal B., Patra S., 2017, Nucl. Phys. A, 966, 197
Kunjipurayil A., Zhao T., Kumar B., Agrawal B. K., Prakash M., 2022, Phys. Rev. D, 106, 063005
Kurkela A., 2010, Phys. Rev. D, 81, 105021
Leung S.-C., 2011, Phys. Rev. D, 84, 107301
Lopes A., 2022, ATLAS and CMS Chase the Invisible with the Higgs Boson. https://home.cern/news/news/physics/atlas-and-cms-chase-invisible-higgs-boson
McDermott S. D., 2012, Phys. Rev. D, 85, 023519
McKeen D., 2018, Phys. Rev. Lett., 121, 061802
Maniatis M., 2010, Int. J. Mod. Phys. A, 25, 3505
Miller M. C. et al., 2019, ApJ, 887, L24
Muñoz C., 2004, Int. J. Mod. Phys. A, 19, 3093
Nelson A. E., Reddy S., Zhou D., 2019, J. Cosmol. Astropart. Phys., 07, 012
Oppenheimer J. R., 1939, Phys. Rev., 55, 374
Panotopoulos G., 2017, Phys. Rev. D, 96, 083004
Planck Collaboration VI, 2020, A&A, 641, A6
Pollack J., Spergel D. N., Steinhardt P. J., 2015, ApJ, 804, 131
Quddus A., Panotopoulos G., Kumar B., Ahmad S., Patra S. K., 2020, J. Phys. G: Nucl. Part. Phys., 47, 095202
Raj N., 2018, Phys. Rev. D, 97, 043006
Rather I. A., Panotopoulos G., Lopes I., 2023, preprint (arXiv:2307.03703)
Ren X.-L., Geng L. S., Camalich J. M., Meng J., Toki H., 2012, J. High Energy Phys., 2012, 73
Rezzolla L., Most E. R., Weih L. R., 2018, ApJ, 852, L25
Routaray P., Mohanty S. R., Das H. C., Ghosh S., Kalita P. J., Parmar V., Kumar B., 2023a, preprint (arXiv:2304.05100)
Routaray P., Das H. C., Pattnaik J. A., Kumar B., 2023b, preprint (arXiv:2307.12748)
Routaray P., Das H. C., Sen S., Kumar B., Panotopoulos G., Zhao T., 2023c, Phys. Rev. D, 107, 103039
Sagun V., Giangrandi E., Dietrich T., Ivanytskyi O., Negreiros R., Providência C., 2023, preprint (arXiv:2306.12326)
Sagunski L., 2018, Phys. Rev. D, 97, 064016
Sen S., Kumar S., Kunjipurayil A., Routaray P., Ghosh S., Kalita P. J., Zhao T., Kumar B., 2023, Galaxies, 11, 60
Shapiro S. L., Teukolsky S. A., 1983, Black Holes, White Dwarfs, and Neutron Stars: The Physics of Compact Objects. Wiley, New York
Spergel D. N. et al., 2003, ApJS, 148, 175
Starkman G. D., 1995, Phys. Rev. Lett., 74, 2623
Steigman G., Turner M. S., 1985, Nucl. Phys. B, 253, 375
Taoso M., Bertone G., Masiero A., 2008, J. Cosmol. Astropart. Phys., 03, 022
Tolman R. C., 1939, Phys. Rev., 55, 364
Tondeur F., Brack M., Farine M., Pearson J., 1984, Nucl. Phys. A, 420, 297
Torres-Rivas A., 2019, Phys. Rev. D, 99, 044014
Vaeth H. M., Chanmugam G., 1992, A&A, 260, 250
Walecka J., 1974, Ann. Phys., 83, 491
Yagi K., 2013, Phys. Rev. D, 88, 023009
Yagi K., Yunes N., 2013, Science, 341, 365
Yagi K., Yunes N., 2017, Phys. Rep., 681, 1
Young R. D., 2013, preprint (arXiv:1301.1765)
Zwicky F., 1933, Helvetica Phys. Acta, 6, 110
Zwicky F., 2009, Gen. Relativ. Gravitation, 41, 207

This paper has been typeset from a TEX/LATEX file prepared by the author.